

IL-6 Controls Leukemic Multipotent Progenitor Cell Fate and Contributes to Chronic Myelogenous Leukemia Development

Damien Reynaud,^{1,2,*} Eric Pietras,^{1,2} Keegan Barry-Holson,^{1,2} Alain Mir,³ Mikhail Binnewies,^{1,2} Marion Jeanne,^{1,2} Olga Sala-Torra,⁴ Jerald P. Radich,⁴ and Emmanuelle Passegué^{1,2,*}

¹The Eli and Edythe Broad Center of Regeneration Medicine and Stem Cell Research

²Division of Hematology/Oncology, Department of Medicine
University of California San Francisco, San Francisco, CA 94143, USA

³Fluidigm Corporation, South San Francisco, CA 94080, USA

⁴Clinical Research Division, Fred Hutchinson Cancer Research Center, Seattle, WA 98109, USA

*Correspondence: reynaud@stemcell.ucsf.edu (D.R.), passegué@stemcell.ucsf.edu (E.P.)

DOI 10.1016/j.ccr.2011.10.012

SUMMARY

Using a mouse model recapitulating the main features of human chronic myelogenous leukemia (CML), we uncover the hierarchy of leukemic stem and progenitor cells contributing to disease pathogenesis. We refine the characterization of CML leukemic stem cells (LSCs) to the most immature long-term hematopoietic stem cells (LT-HSCs) and identify some important molecular deregulations underlying their aberrant behavior. We find that CML multipotent progenitors (MPPs) exhibit an aberrant B-lymphoid potential but are redirected toward the myeloid lineage by the action of the proinflammatory cytokine IL-6. We show that BCR/ABL activity controls *Il-6* expression thereby establishing a paracrine feedback loop that sustains CML development. These results describe how proinflammatory tumor environment affects leukemic progenitor cell fate and contributes to CML pathogenesis.

INTRODUCTION

Chronic myelogenous leukemia (CML) is a clonal myeloproliferative neoplasm (MPN) characterized by the t(9;22)(q34;q11) reciprocal translocation, which leads to the expression of the *BCR/ABL* fusion protein (Savona and Talpaz, 2008). *BCR/ABL* is a hyperactive and deregulated tyrosine kinase that promotes leukemic growth by disrupting a broad range of signaling pathways involved in cell survival, proliferation, and differentiation. Clinically, the natural course of the disease includes three distinct phases (Perrotti et al., 2010). The initial phase is characterized by a progressive myeloid expansion, with accumulation of myeloid progenitors and mature granulocytes in the bone marrow (BM) and peripheral blood (PB). Upon acquisition of secondary mutations, this chronic phase evolves through an accelerated phase into an acute leukemia-like blast crisis involving

either myeloid, B lymphoid or myeloid/lymphoid biphenotypic cells. During the chronic phase, CML cells have been shown to be functionally heterogeneous and capable of maintaining a hierarchical organization caricaturing normal hematopoiesis, with only a fraction of the cells being actually responsible for disease maintenance and propagation, thus behaving as leukemia-initiating stem cells (LSCs) (Passegué and Weisman, 2005).

The existence of a LSC compartment has fundamental consequences for CML therapy (Savona and Talpaz, 2008). Although *BCR/ABL* tyrosine kinase inhibitors (TKIs) are remarkably effective in inducing remission in chronic phase patients, they are not effective against CML-LSCs, which can persist and regenerate the disease upon drug discontinuation. Why CML-LSCs are refractory to TKIs remains a matter of debate. One explanation could be a failure to achieve an efficient therapeutic concentration of TKIs in CML-LSCs due to their particular location in

Significance

Here, we show that the clinically relevant CML-LSCs are solely contained in the LT-HSC compartment, and identify aberrant features of these cells that could be amenable to targeted therapy. We find that CML-LSCs are hyperproliferative and out compete normal LT-HSCs due to major alterations in their cell cycle control and deregulation of the Notch pathway. Moreover, we identify two leukemic progenitors, which are devoid of self-renewal activity but are critical for CML pathogenesis. We demonstrate that *BCR/ABL* controls expression of the proinflammatory cytokine IL-6 and establishes a paracrine loop acting on leukemic MPPs to promote myeloid development at the expense of lymphoid differentiation. This finding adds IL-6 blocking therapy as a potential strategy to control CML development.

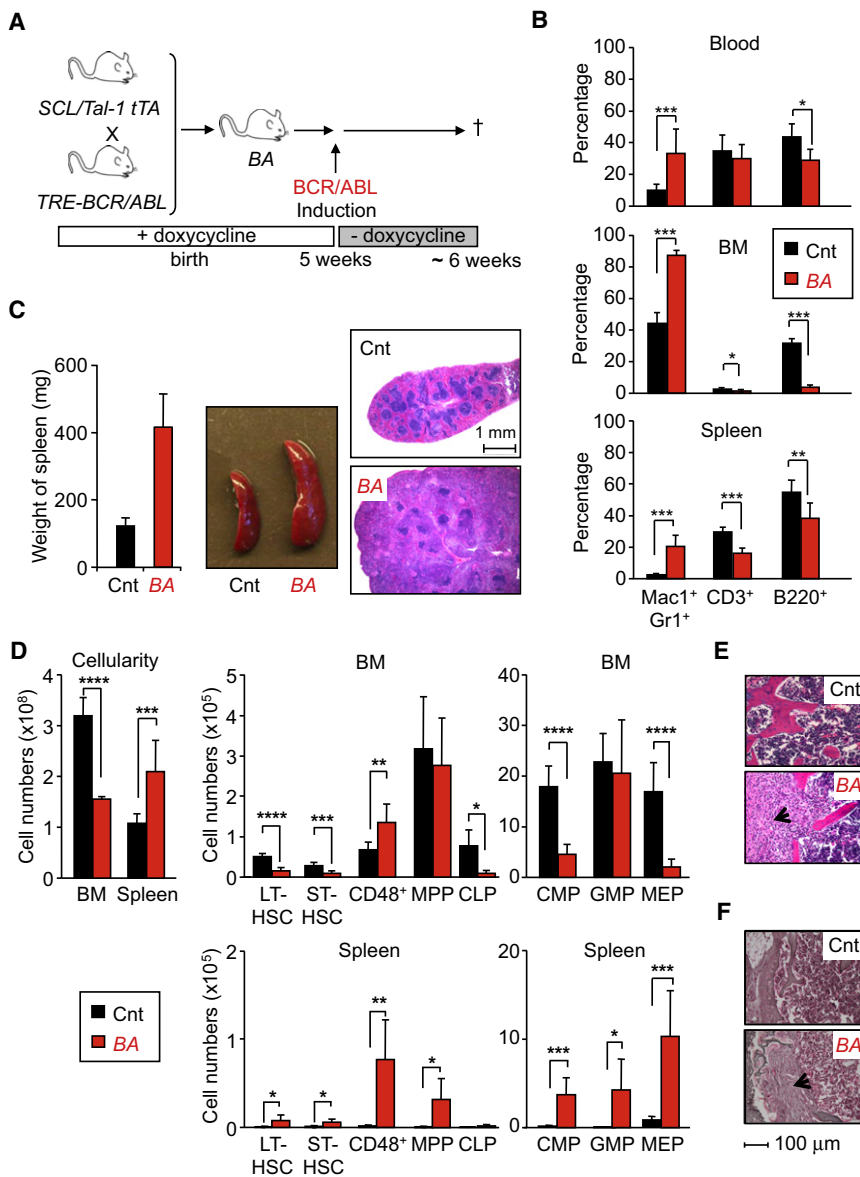


Figure 1. CML Hematopoiesis in Inducible BCR/ABL Transgenic Mice

(A) Experimental scheme. Double transgenic mice (BA) were maintained in presence of doxycycline (20 mg/l) in drinking water until 5 weeks of age before inducing *BCR/ABL* by doxycycline withdrawal. WT and single transgenic littermates treated with the same regimen were used as controls (Cnt) and all the mice were analyzed 6 weeks after doxycycline withdrawal.

(B) Hematopoietic features in CML mice. Graphs show the percentages of mature cells detected in PB, BM, and spleen of Cnt and BA mice. Results are expressed as mean \pm SD ($n \geq 8$; * $p \leq 10^{-2}$, ** $p \leq 10^{-3}$, *** $p \leq 10^{-4}$).

(C) Weight, morphology and hematoxylin and eosin (H&E) staining of spleen from Cnt and BA mice.

(D) Total cellularity and cell number for each progenitor compartment in BM and spleen of Cnt and BA mice. Results are expressed as mean \pm SD ($n \geq 6$; * $p \leq 10^{-2}$, ** $p \leq 10^{-3}$, *** $p \leq 10^{-4}$, **** $p \leq 10^{-5}$).

(E) H&E staining of BM (sternum) section from Cnt and BA mice. The arrowhead indicates myelofibrotic tissue.

(F) Gordon and Sweet's reticulin staining of BM (sternum) section from Cnt and BA mice. The arrowhead indicates myelofibrotic tissue. See also Figure S1.

stem cell (HSC) enriched Lin⁻/Sca-1⁺/c-Kit⁺ (LSK) fraction of the BM (Hu et al., 2006), and that developmental pathways controlling HSC function are essential for CML-LSCs generation and CML development (Warr et al., 2011). However, such experimental approaches have inherent limitations due to the constraints imposed by the retroviral transduction, and the use of irradiated recipients for transplantation. In this context, the *Scf/Tal1-tTA x TRE-BCR/ABL* double transgenic mice, which allow for inducible

BCR/ABL expression in HSCs and CML development in adult mice (Koschmieder et al., 2005), represent a valuable alternative to study CML pathogenesis and to test therapies in vivo (Zhang et al., 2010). Here, we used this inducible *BCR/ABL* transgenic mouse model to understand the effect of *BCR/ABL* activity on hematopoietic development.

RESULTS

CML Development Is Associated with a Profound Reorganization of BM Hematopoiesis

Scf/Tal1-tTA and *TRE-BCR/ABL* transgenic mice were bred in the presence of doxycycline, and *BCR/ABL* (BA⁺) expression was induced by doxycycline withdrawal 5 weeks after birth (Figure 1A). All induced double transgenic mice (thereafter called BA mice) progressively developed a CML-like disease associated with a severe myeloid cell expansion and reduction in B and

protective niches, their high content of drug efflux pumps and/or their enhanced expression of *BCR/ABL* (Barnes and Melo, 2006). A recent study suggests an alternative scenario wherein CML-LSCs are not killed by TKIs as other CML cells because they are actually insensitive to *BCR/ABL* inhibition (Corbin et al., 2011). This model predicts that *BCR/ABL*-based therapies will not eliminate CML-LSCs and highlights the need for approaches targeting alternative pathways that are critical for LSCs maintenance. A refined characterization and better understanding of CML-LSC biology is therefore essential for the establishment of targeted anti-LSC therapies and the development of curative treatment for CML.

Historically, *BCR/ABL* retroviral transduction/transplantation studies in the mouse have been instrumental in showing that *BCR/ABL* is the direct cause of CML and in validating this oncogene as a drug target. Furthermore, these studies were used to demonstrate that CML-LSCs are contained in the hematopoietic

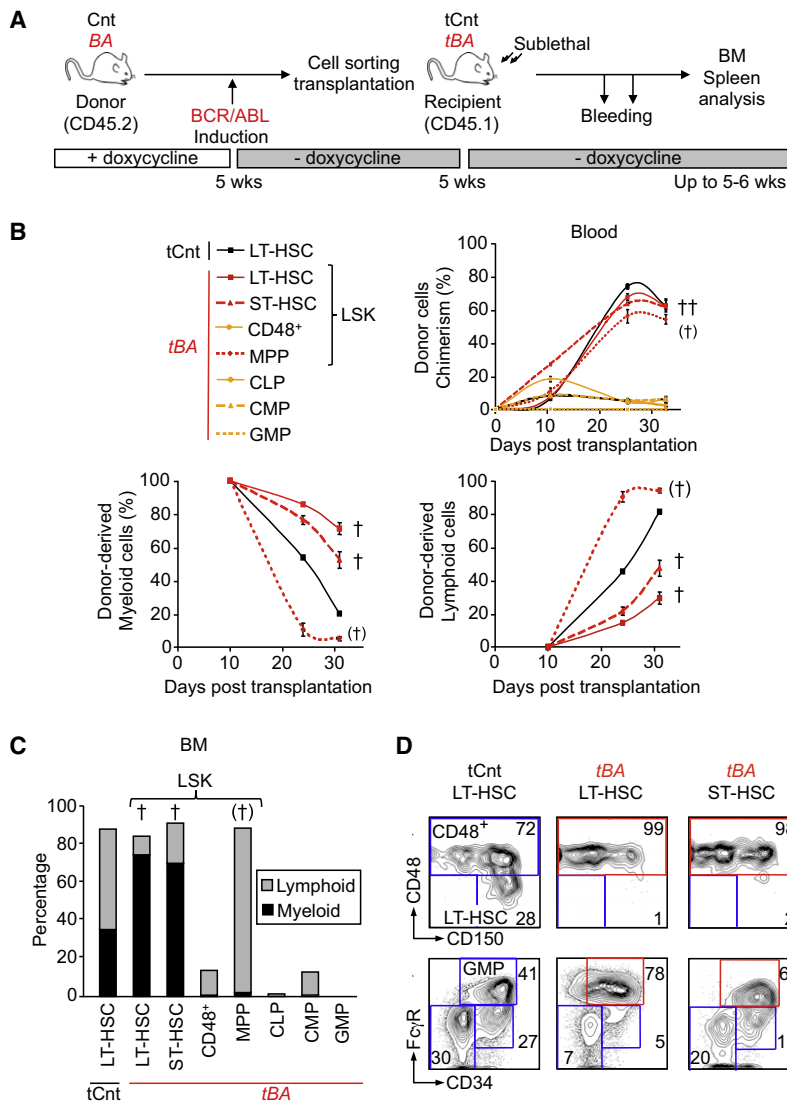


Figure 2. Refining the Identity of CML Leukemic Stem Cells

(A) Experimental scheme. Cells were isolated by flow cytometry from Cnt or BA mice (CD45.2) 5 weeks after doxycycline withdrawal. Four thousand (LT-HSC, ST-HSC, CD48⁺, MPP, and CLP) or 40,000 (CMP and GMP) cells were transplanted into sublethally irradiated CD45.1 recipients (denoted tCnt and tBA). Transplanted mice were bled at several time points, and BM analyses were performed at 35 days posttransplantation.

(B) Kinetics of hematopoietic reconstitution in PB. The upper graph indicates the overall percentage of CD45.2 chimerism. The lower left and right graphs show the percentage of donor-derived myeloid (Mac1⁺) and lymphoid (B220⁺/CD3⁺) cells, respectively. Results are expressed as mean \pm SEM (n = 2–6). †, Cohort with partial mortality (two out of seven).

(C) Hematopoietic reconstitution in BM. Histograms show the average percentage (n = 2–5) of donor-derived myeloid (Mac1⁺, black) and lymphoid (B220⁺/CD3⁺, gray) cells.

(D) Reorganization of the immature BM compartments in transplanted mice. Representative FACS plots showing the change in frequency in mice transplanted with 4000 Cnt or BA⁺ LT-HSCs and ST-HSCs. See also Figure S2.

T cell lineages in the BM, spleen and PB (Figures 1A and 1B; see Figure S1A available online), and splenomegaly (Figure 1C). BA mice also became moribund ~6 weeks after induction. In contrast to other genetic backgrounds (Koschmieder et al., 2005), no lymphoid disorders were observed in over 100 BA mice on a pure C57Bl/6 background. CML development in 5–6-weeks-induced BA mice was associated with a 2-fold reduction in BM cellularity (Figure 1D) and the development of a profound myelofibrosis (Figures 1E and 1F), as previously described in ~30% of CML patients (Buesche et al., 2007). Analysis of the LSK compartment showed a severe reduction in the number of LT-HSCs (LSK/Fik2[−]/CD48[−]/CD150⁺) and ST-HSCs (LSK/Fik2[−]/CD48[−]/CD150[−]), which was accompanied by an expansion of the nonself-renewing CD48⁺ cells (LSK/Fik2[−]/CD48⁺), whereas the number of MPPs (LSK/Fik2⁺) remained unchanged (Figure 1D; Figure S1B). Analysis of the myeloid progenitor compartment indicated a severe reduction in the number of common myeloid progenitors (CMP: LK/CD34⁺/FcγR[−]) and megakaryocyte/erythrocyte progenitors (MEP: LK/CD34[−]/FcγR[−]), whereas the

number of granulocyte/macrophage progenitors (GMP: LK/CD34⁺/FcγR⁺) remained unchanged and fueled CML development (Figure 1D; Figure S1B). Finally, the reduction in lymphoid-lineage cells was correlated with a ~8-fold decrease in the number of common lymphoid progenitors (CLP: Lin[−]/c-Kit^{low}/Sca1^{low}/Fik2⁺/IL7Rα⁺) (Figure 1D). These BM changes were also associated with the development of an extramedullary hematopoiesis in the spleen affecting all immature compartments, except for CLPs (Figures 1C and 1D). Altogether, these results indicate a profound hematopoietic remodeling in response to CML development characterized by the loss of the

immature stem and progenitor compartments in the BM, and their compensatory increase and redistribution to peripheral organs.

BCR/ABL Alters the Biology of Several Stem and Multipotent Progenitor Cells

To assess how BCR/ABL activity affects the biological output of specific BM populations, we transplanted highly purified stem and progenitor cells isolated from 5–6-weeks-induced BA mice into sublethally irradiated congenic recipients (Figure 2A). As expected, transplantation of BA⁺ myeloid-committed CMPs and GMPs (Huntly et al., 2004), but also of lymphoid-committed CLPs, failed to sustain lasting chimerism in the PB, BM and spleen and to transplant the disease (Figures 2B and 2C; Figure S2A). Similarly, transplantation of the two most abundant populations present in the LSK compartment (i.e., MPPs and the expanded CD48⁺ cells) failed to transfer CML, although transplantation of BA⁺ MPPs led to a high degree of chimerism due to a massive production of B cells (Figure S2B). In contrast,

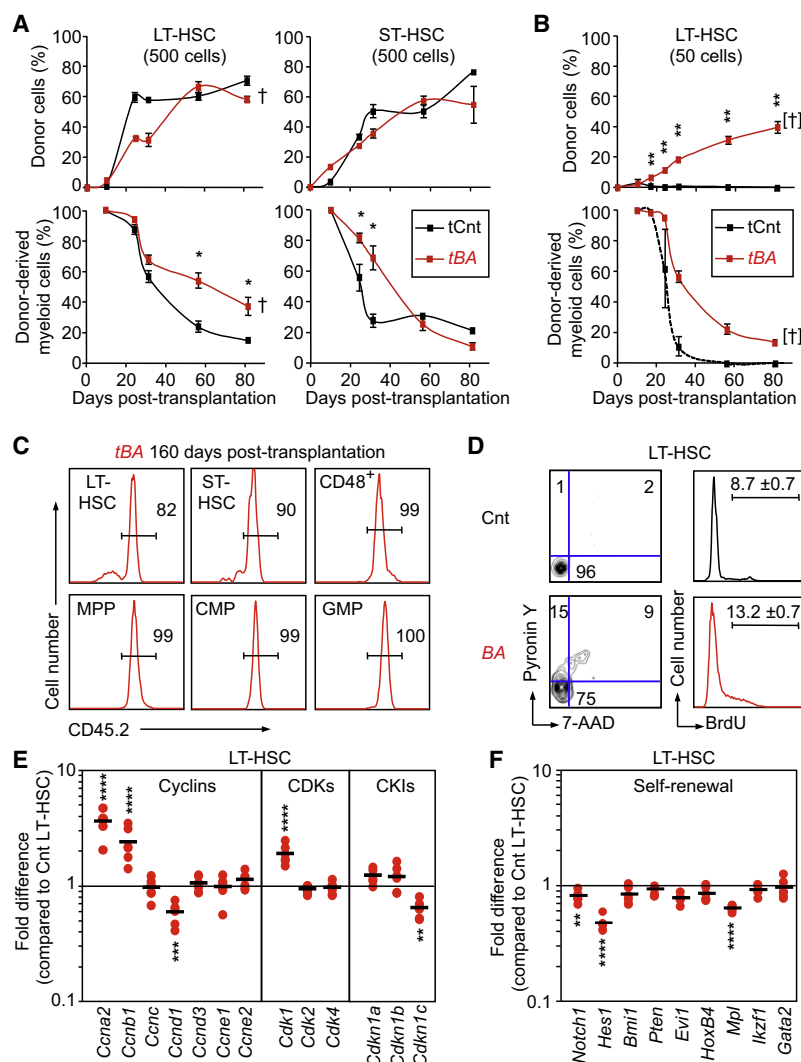


Figure 3. Functional and Molecular Characterization of CML Leukemic Stem Cells

(A) Leukemic potential of CML LT-HSCs and ST-HSCs. Cells were isolated from Cnt and BA mice (CD45.2) 5 weeks after doxycycline withdrawal and transplanted (500 cells/mouse) into sublethally irradiated recipients (CD45.1). Transplanted mice were bled at several time points and analyzed for overall percentage of CD45.2 chimerism (upper graphs) and percent of donor-derived Mac1⁺ myeloid cells (lower graphs). Results are expressed as mean \pm SEM ($n = 2-3$; $^{*}p \leq 5 \times 10^{-2}$). †Indicates cohorts found moribund.

(B) Limiting dilution transplantation. Fifty Cnt or BA⁺ LT-HSCs (CD45.2) were transplanted into sublethally irradiated recipients (CD45.1) together with 3×10^5 Sca-1-depleted BM cells (CD45.1). Graphs show kinetics of hematopoietic reconstitution in PB and results are expressed as mean \pm SEM ($n = 7$; $^{*}p \leq 10^{-3}$). †Indicates cohort found moribund at later time points.

(C) Clonal expansion analyses. The panels show representative examples of the percentage of CD45.2 chimerism in BM compartments 160 days after transplantation of 50 BA⁺ LT-HSCs.

(D) Cell-cycle analyses. LT-HSCs were isolated from Cnt and BA mice 5 weeks after doxycycline withdrawal. The left panels show DNA/RNA contents analyzed by 7-AAD and Pyronin Y staining, and the right panels show BrdU incorporation in cells cultured for 1 hr with 60 μ M BrdU. Results are expressed as mean \pm SEM ($n = 2$).

(E and F) Quantitative gene expression analyses. Pools of 100 Cnt and BA⁺ LT-HSCs were analyzed on a Fluidigm Dynamic Array IFC for a custom made set of cell cycle and self-renewal genes, respectively. Results are expressed as fold change relative to Cnt LT-HSCs ($n = 7$; $^{*}p \leq 10^{-3}$, $^{***}p \leq 10^{-4}$, $^{****}p \leq 10^{-5}$).

transplantation of either BA⁺ LT-HSCs or ST-HSCs (4000 cells/mouse) both induced the development of a robust CML disease, with the transplanted mice becoming moribund within 1 month posttransplantation (Figure 2B). Analyses of these mice showed a clear bias toward myeloid cell production in the BM, spleen, and PB (Figure 2C; Figures S2A and S2B), together with a severe reorganization of the stem and progenitor compartments in the BM (i.e., increased percentage of CD48⁺ cells and GMPs) (Figure 2D), infiltration of mature myeloid cells in the liver (Figure S2C), and development of splenic extramedullary hematopoiesis (data not shown). Taken together, these results show that transplantation of either LT-HSCs or ST-HSCs recapitulates the core features of the CML disease observed in primary BA mice, and suggest that two distinct stem cell populations present in the LSK compartment may function as LSCs, at least at high doses of transplanted cells.

Refining the Identity of CML-LSCs

LT- and ST-HSCs are functionally defined by the extent of their self-renewal capacity (Benveniste et al., 2010). To investigate how such functional distinctions translated in the context of

CML leukemogenesis, we performed transplantation in limiting conditions into sublethally irradiated recipients (Figure 3A). Although transplantation of either 500 control or BA⁺ LT-HSCs or ST-HSCs gave rise to similar levels of PB chimerism, only BA⁺ LT-HSCs maintained an elevated production of myeloid cells that ultimately led to CML development and death of the recipient mice (93 ± 6 days; $n = 3$). In contrast, BA⁺ ST-HSCs only promoted a transient myeloid hyperplasia that resulted in the same percentage of circulating myeloid cells than control ST-HSCs by 50 days posttransplantation. We also transplanted 50 control or BA⁺ LT-HSCs into sublethally irradiated recipients to better quantify the number of CML-LSCs present in the LT-HSC compartment (Figure 3B). Although we did not observe significant engraftment from control LT-HSCs under these highly competitive conditions, six of the seven mice transplanted with 50 BA⁺ LT-HSCs showed a robust ($37.9 \pm 4.5\%$) and long-lasting (>20 weeks) multilineage PB chimerism. Moreover, five of the six engrafted mice developed CML and become moribund with a latency of 159 ± 24 days, indicating that one out of 40 BA⁺ LT-HSCs (calculated according to Poisson statistics, data not shown) is a bona fide CML-LSC. Strikingly, BM analysis of diseased mice showed that CML-LSCs were able to completely out-compete the normal hematopoiesis re-emerging from irradiated recipients (Figure 3C). Altogether, these results demonstrate that CML-LSCs reside exclusively within the LT-HSC

compartment and display a massive competitive advantage at the clonal level. They also indicate that BA^+ ST-HSCs function as a short-term leukemic progenitor compartment, which amplifies the myeloid hyperplasia in a manner that might eventually be fatal upon transplantation of large numbers of cells, but which cannot per se sustain long-term CML development.

Aberrant Features and Molecular Deregulations in CML-LSCs

We next investigated how BCR/ABL impacts on the molecular networks controlling LT-HSC function. We observed a striking hyperproliferative phenotype in BA^+ LT-HSCs (Figure 3D), which was characterized by a significant loss of quiescence and a 2-fold increase in proliferation rates. We then used a Fluidigm Dynamic RT-PCR array to perform a detailed quantitative expression analysis of 96 genes of interest in pools ($n = 7$) of 100 control and BA^+ LT-HSCs (Figure 3F). Consistent with their increased proliferation, expression of the G₂/M cyclins A2 (*Ccna2*) and B1 (*Ccnb1*), and their associated cyclin-dependent kinase 1 (*Cdk1*), was elevated in BA^+ LT-HSCs. We also observed decreased expression of the early G₁ cyclin D1 (*Ccnd1*) and cyclin-dependent kinase inhibitor p57 (*Cdkn1c*) in BA^+ LT-HSCs, similar to what we have already reported in another population of LT-HSC-derived LSCs in *junB*-deficient CML-like mice (Santaguida et al., 2009). Focusing on self-renewal programs, we confirmed the previously described downregulation of *Evi1* and *Mpl* expression in BA^+ LT-HSCs (Schemionek et al., 2010), and found no significant changes in the expression levels of *Bmi1*, *Pten*, *Hoxb4*, *Ikzf1* (*Ikars*), and *GATA2* (Figure 3G). Strikingly, we uncovered major alterations in the regulation of the Notch pathway, with significant reduction in the expression of both *Notch1* and its transcriptional target *Hes1* in BA^+ LT-HSCs. Taken together, these results indicate that CML-LSCs have a hyperproliferative phenotype that occurs without loss of self-renewal activity, and leads to clonal dominance. They also suggest that impairment of the Notch signaling pathway could contribute to the aberrant proliferation and myeloid cell production from CML-LSCs as previously reported for *junB*-deficient LSCs (Santaguida et al., 2009) and more recently described in other MPN models (Klinakis et al., 2011).

Transient B Cell Hyperplasia Arising from Leukemic MPPs

Although both BA^+ LT-HSCs and ST-HSCs have an extensive ability to produce myeloid cells, transplantation of BA^+ MPPs promotes a surprising B cell overproduction (Figures 2B and 2C; Figure S2B). To better understand this phenomenon, we transplanted control or BA^+ MPPs (4000 cells/mouse) into sublethally irradiated recipients (Figure 4A). Analyses performed at 35 days posttransplantation showed dramatically elevated BM chimerism in mice transplanted with BA^+ MPPs compared to control MPPs, which consisted mainly of B220⁺ donor-derived B cells and reflected a specific increase in CD43⁺ pro-B cells with corresponding decreased in CD43⁺ pre-B and IgM⁺ immature/mature B cells (Figure 4B). This massive increase in pro-B cell production from BA^+ MPPs was able to completely repress hematopoietic recovery from sublethally irradiated recipient mice (Figure S3A). Consistent with this major hematopoietic disruption, two out of seven transplanted mice were anemic

and moribund when analyzed, whereas the other mice developed extensive splenic extramedullary hematopoiesis and survived (data not shown). This pro-B cell hyperplasia was specific to the leukemic MPP compartment, as the output of the downstream CLP compartment was not similarly affected by BCR/ABL activity (Figure 2C and data not shown). In addition, it did not correspond to the development of B cell acute lymphoblastic leukemia (B-ALL), as the pro-B cell hyperplasia remained restricted to the BM (Figures S3B and S3C) and was not transplantable to secondary recipients (data not shown). Most notably, this hyperplasia did not persist over time and was absent in the surviving mice by 70 days posttransplantation (Figure 4B). Altogether, these results indicate that BCR/ABL increases and biases the differentiation potential of MPPs toward the production of B cell progenitors at the expense of myeloid cell generation, but without promoting its oncogenic transformation.

Context-Dependent Behavior of Leukemic MPPs

Although we observed an extensive B-lymphoid potential in transplanted BA^+ MPPs, primary BA mice displayed a reduced B cell compartment (Figure 1B). To address this paradox, we cotransplanted 4000 BA^+ MPPs together with 4000 BA^+ HSCs (either long-term or short-term) into sublethally irradiated recipients (Figure 4C). Strikingly, 35 days after cotransplantation, four out of five recipient mice developed a CML disease (Figure 4C), which indicated that pathological myeloid expansion driven by BA^+ HSCs was able to repress the B cell expansion promoted by leukemic MPPs. We then analyzed the biological properties and molecular regulation of MPPs isolated from primary CML-developing BA mice. Consistent with their extensive reconstitution activity upon transplantation, BA^+ MPPs exhibit a 2-fold increase in proliferation rates (Figure 4D). Gene expression analyses of BA^+ MPPs only revealed marginal changes for genes encoding cell cycle regulators (Figure S3D). In contrast we observed a striking increase in the expression levels of myeloid determinants such as *Irf8* or *Csf1r* (*M-CSFR*), and a concomitant decrease in the expression of key lymphoid determinants including *Notch1*, *Hes1*, *Gfi1*, *Ikzf1* (*Ikars*), and *Tcf3* (*E2A*) in BA^+ MPPs (Figure 4E). Taken together, these results indicate that BA^+ MPPs are intrinsically poised toward B lymphoid differentiation but are reprogrammed toward the myeloid fate during CML development, hence revealing an unexpected context-dependent behavior for these leukemic MPPs.

CML-Driven IL-6 Production Suppresses Lymphoid Differentiation from Leukemic MPPs

We reasoned that molecular effectors responsible for the fate reprogramming of leukemic MPPs could be extracellular signaling molecules detectable in the serum of CML-developing mice. Analyses performed with an antibody-based protein array revealed increased levels of a number of cytokines and growth factors in the serum of primary BA mice (Figure 5A). We focused on the multifunctional proinflammatory cytokine interleukin-6 (IL-6), which has been previously implicated in both myeloid expansion and lymphocytopenia (Maeda et al., 2005). Using an enzyme-linked immunosorbent assay (ELISA) on sera and spleen homogenates, we confirmed increased IL-6 concentrations in all CML-developing mice, either primary BA mice or BA^+ HSCs transplanted mice (Figure 5B). qRT-PCR analyses

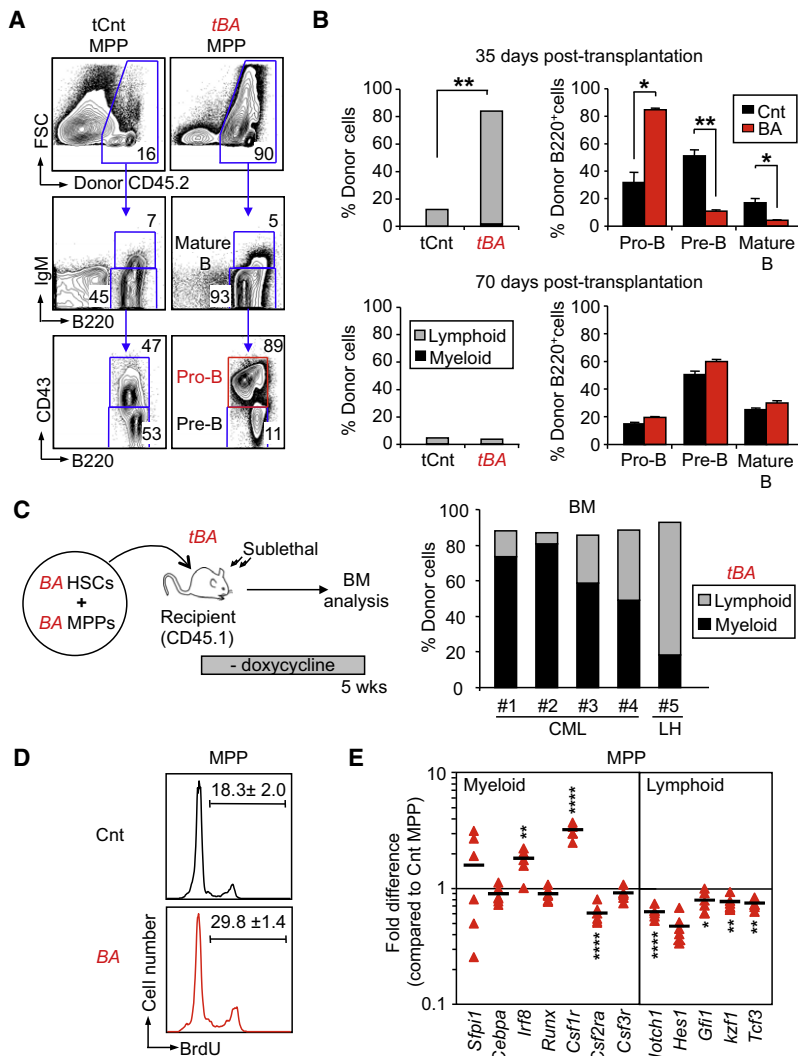


Figure 4. Context-Dependent Behavior of Leukemic MPPs

(A) Reconstitution potential of CML MPPs. Four thousand Cnt or BA⁺ MPPs (CD45.2) were transplanted into sublethally irradiated recipient mice (CD45.1). Recipients (n = 5) were sacrificed and BM reconstitution was analyzed by flow cytometry 35 days posttransplantation. Representative FACS plots showing an example of B cell progenitor reconstitution.

(B) Kinetics of B cell production in recipient BM at 35 (top panels) and 70 (bottom panels) days posttransplantation. The left graphs indicate the average percentage of donor-derived myeloid (Mac1⁺, black) and lymphoid (B220⁺/CD3⁺, gray) cells. The right graphs show the percentage of CD43⁺/IgM⁺ pro-B, CD43⁺/IgM⁺ pre-B and IgM⁺ mature B cells in the donor-derived B220⁺ cells. Results are expressed as mean ± SEM (n = 2–5; *p ≤ 5 × 10^{−2}, **p ≤ 5 × 10^{−3}).

(C) In vivo competition between leukemic compartments. Four thousand BA⁺ HSCs (either LT-HSCs or ST-HSCs) together with 4000 BA⁺ MPPs (both CD45.2) were co-transplanted into sublethally irradiated recipient mice (CD45.1). The right graph shows the percentage of donor-derived myeloid and lymphoid cells in the BM of recipient mice 35 days posttransplantation. Of note, four of five mice developed a myeloid disease (CML) and one mouse a lymphoid hyperplasia (LH).

(D) Cell-cycle distribution. BrdU incorporation in MPPs isolated from Cnt and BA mice 5 weeks after doxycycline withdrawal and cultured for 1 hr with 60 μM BrdU. Results are expressed as mean ± SEM (n = 2).

(E) Quantitative gene expression analyses. Pools of 100 Cnt and BA⁺ MPPs were analyzed on a Fluidigm Dynamic Array IFC for a custom made set of genes regulating myeloid versus lymphoid lineage specification. Results are expressed as fold change relative to Cnt MPPs (n = 7; *p ≤ 10^{−2}, **p ≤ 10^{−3}, ***p ≤ 10^{−5}). See also Figure S3.

demonstrated that the expanded myeloid CML cells were the major source of IL-6 production during disease development (Figure 5C), whereas flow cytometry studies indicated that the receptor for IL-6 (IL-6Rα) was detectable on both control and BA⁺ MPPs and downstream myeloid progenitors, but not on the most immature LT-HSCs or ST-HSCs (Figure 5D). Strikingly, addition of murine recombinant IL-6 completely blocked the ability of BA⁺ MPPs to generate CD19⁺ B cells in vitro (Figure 5E). In addition, IL-6 dramatically increased the numbers and size of myeloid colonies generated from BA⁺ MPPs in methylcellulose clonogenic assays, whereas no significant effects were observed from BA⁺ GMP in the same conditions (Figure 5F). Taken together, these results indicate that the IL-6 secreted by the expanded myeloid CML cells directly acts on leukemic MPPs and redirects their aberrant *BCR/ABL*-driven intrinsic B cell potential toward the myeloid lineage (Figure 5G).

In Vivo Cross-Talk between Leukemic and Nonleukemic Hematopoietic Compartments

In CML patients, the leukemic cells coexist and compete with normal hematopoiesis. To model such interactions and validate

the function of IL-6 in these relevant conditions, we cotransplanted 2 × 10⁶ wild-type (WT: CD45.2 GFP⁺) along with 2 × 10⁶ noninduced BA (CD45.2 GFP[−]) unfractionated BM cells into lethally irradiated recipients (CD45.1 GFP[−]) maintained under doxycycline (Figure 6A). As expected, WT and noninduced BA cells showed a similar 50:50 chimerism at 2 months posttransplantation (Figure 6B). Upon doxycycline withdrawal, four of five transplanted mice developed CML with disease onset ranging from 40 to 154 days (median 99 days; n = 4). Strikingly, the 50:50 chimerism was preserved in CML-developing mice, with both WT and BA⁺ cells contributing to the expanded mature myeloid cells (Figure 6B). We also confirmed increased concentrations of IL-6 in the serum of CML-developing mice (Figure 6C). Interestingly although BA⁺ cells were overrepresented within the LT-HSC and ST-HSC compartments (85.8% ± 5.1 and 82.4% ± 6.1 respectively; mean ± SEM; n = 2), the MPP compartment displayed an equal contribution of BA⁺- and WT-derived cells (50.9% ± 1.3 BA⁺ cells, mean ± SEM, n = 2) similar to the 50:50 chimerism found in the expanded myeloid lineage. Taken together, these results confirm in vivo that lineage determination can be controlled by systemic factors downstream of CML-LSCs, and correlate the increase in IL-6 production driven by myeloid CML cells with the

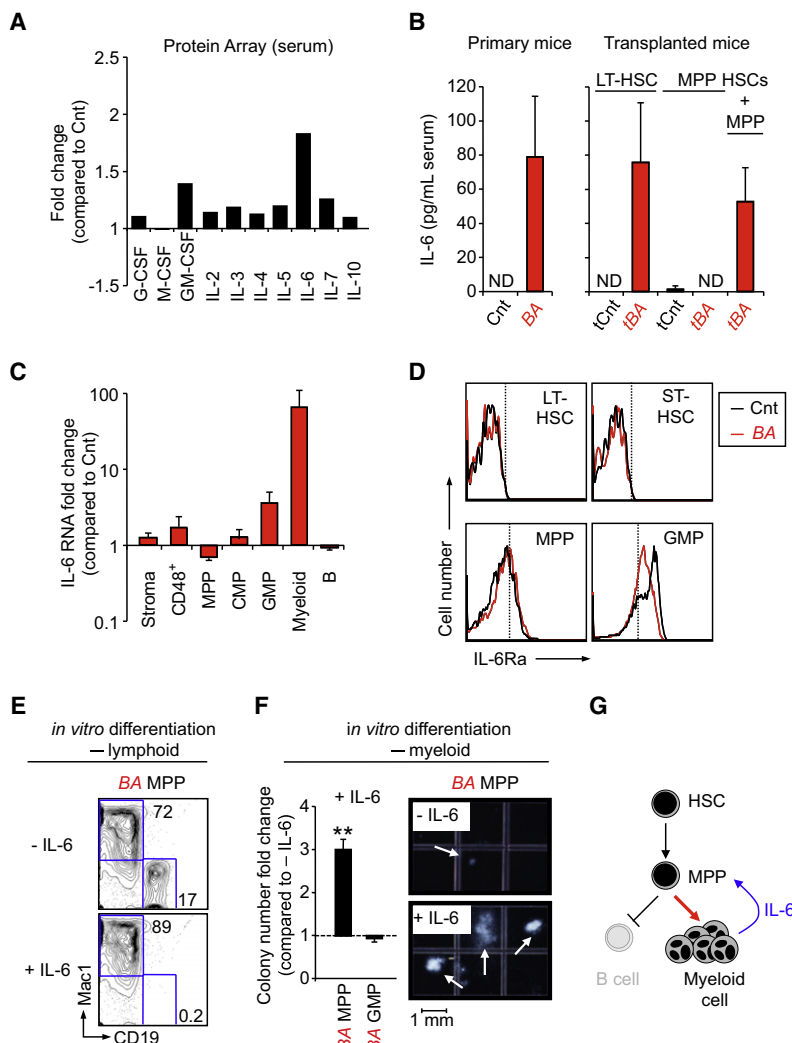


Figure 5. IL-6 Paracrine Loop

(A) Protumorigenic inflammatory environment during CML development. Changes in the indicated growth factor and interleukin levels were determined using an antibody-based protein array on pools of sera from 16 Cnt and 7 BA mice 6 weeks after doxycycline withdrawal. Results are expressed as fold change relative to levels measured in Cnt mice (set to 1).

(B) Modulation of serum IL-6 levels. ELISA measurement of IL-6 concentration in serum of individual Cnt and BA primary mice (left graphs), and mice transplanted with the indicated populations (right graphs). Results are expressed as mean \pm SEM ($n = 2-6$). ND, not detectable.

(C) qRT-PCR analysis of nonhematopoietic BM cells (stroma), CD48⁺, MPP, CMP, GMP, mature myeloid, and B cells for *Il-6* mRNA levels. Results are expressed as mean \pm SEM ($n = 3$).

(D) Representative FACS histograms showing expression of the α chain of IL-6 receptor on the indicated Cnt (black) and BA⁺ (red) populations. Dashed lines show isotype control negative boundaries. Data are representative of two independent experiments.

(E) Effect of IL-6 on lymphoid differentiation from BA⁺ MPPs. The FACS plots show a representative phenotypic analysis of CD19 (lymphoid) and Mac-1 (myeloid) markers after 8 days of *in vitro* culture ($n = 2$).

(F) Differential effect of IL-6 on myeloid differentiation from BA⁺ MPPs and GMPs. The graph on the left shows the fold changes in colony numbers when comparing conditions with or without IL-6 (set to 1). Results are expressed as mean \pm SEM ($n = 2-3$; $^{**}p \leq 5 \times 10^{-4}$). The photographs on the right show representative myeloid colonies generated in both conditions from BA⁺ MPPs after 10 days of *in vitro* culture.

(G) Model describing the IL-6 paracrine loop in CML development identified in this study.

re-routing of both leukemic and normal MPPs toward the myeloid lineage.

IL-6 Contributes to CML Development

To confirm the function of IL-6 in CML pathogenesis, we evaluated disease progression in the absence of IL-6 signaling by crossing BA mice with *Il-6*^{-/-} mice (Kopf et al., 1994). Upon doxycycline withdrawal, both BA *Il-6*^{-/-} and BA *Il-6*^{+/-} mice displayed significantly increased overall survival compared to BA *Il-6*^{+/+} mice (Figure 7A). Consistent with IL-6 serum concentrations (Figure 7B), we observed a stepwise decreased in myeloid cell production together with a stepwise recovery of B cell generation in the BM of BA *Il-6*^{+/-} and *Il-6*^{-/-} mice (Figure 7C). These effects were specific to *Il-6* inactivation because disruption of other cytokine signaling pathways, such as GM-CSF signaling, in BA mice did not affect CML development (data not shown). Interestingly, the lymphoid restoration observed in BA *Il-6*^{-/-} mice also displayed aberrant pro-B cell features (Figure 7C) similar to the pro-B cell expansion observed upon transplantation of purified BA⁺ MPPs (Figure 3B). In addition, BA *Il-6*^{-/-} mice maintained a high level of myeloid cells

circulating in the PB due to their extensive extra-medullary hematopoiesis (data not shown), and eventually succumb to late onset CML diseases without developing overt lymphoid malignancies. Altogether, these results demonstrated that IL-6 signaling normally blocks the aberrant *BCR/ABL*-driven pro-B cell potential of leukemic MPPs and enhances myeloid differentiation, hence leading to a positive feedback loop promoting CML development. They also indicate that IL-6 blocking strategy can significantly delay CML onset in situations where *BCR/ABL* remains active.

BCR/ABL Controls *Il-6* Expression in Myeloid CML Cells

Finally, we investigated the mechanisms controlling IL-6 production using human leukemic cell lines and samples from CML patients. *BCR/ABL*-expressing K562 erythro-leukemic cells and HL60 promyelocytic leukemia cells engineered to stably express *BCR/ABL* (Porosnicu et al., 2001) displayed high levels of *Il-6* mRNA, which could be rapidly downregulated by inhibition of *BCR/ABL* activity with TKIs (Imatinib or Dasatinib) (Figure 8A). This effect was specific to *Il-6* because the expression of *BCR/ABL* and other components of the IL-6 signaling pathway, including *IL-6Ra*, were not similarly affected by TKI treatment. For both cell lines, ELISA analyses confirmed that changes in *Il-6* gene expression correlated with changes in the levels of

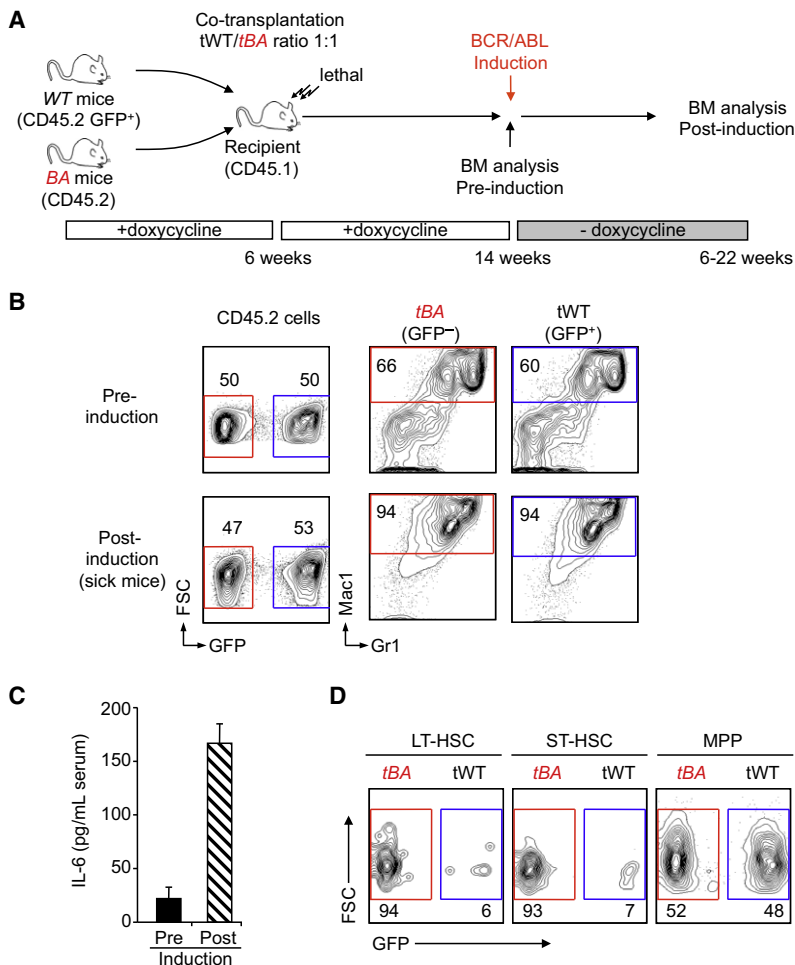


Figure 6. Contribution of IL-6 to Lineage Determination In Vivo

(A) Experimental scheme where 5×10^6 wild-type (tWT: CD45.2 GFP⁺) and 5×10^6 noninduced BA⁺ (tBA: CD45.2 GFP⁻) BM cells were cotransplanted into lethally irradiated recipients (CD45.1). Transplanted mice were maintained on doxycycline for 2 months to achieve stable reconstitution before inducing BA expression by doxycycline withdrawal. Mice were analyzed either pre- or post-BA-induction, when mice displayed signs of CML disease.

(B) Representative FACS plots showing contribution of tWT and tBA cells to the myeloid (Mac1⁺/Gr1⁺) BM output pre (top) and post (bottom) induction ($n \geq 2$).

(C) Concentration of IL-6 in the serum of transplanted mice pre- and postinduction. Results are expressed as mean \pm SEM ($n = 2-4$).

(D) Representative FACS plots showing contribution of tWT and tBA cells to the indicated BM compartments postinduction ($n = 2$).

in *BCL6* expression, particularly in blast crisis samples (Figure 8E), whereas upregulation of *LIN28* during CML progression has been previously reported (Viswanathan et al., 2009). Taken together, these results demonstrate that BCR/ABL activity controls *IL-6* expression in myeloid CML cells, and suggest that both *BCL6* and *LIN28/28b* are involved in the complex molecular network mediating this effect.

DISCUSSION

In this study, we use an inducible *BCR/ABL* transgenic mouse model that recapitulates the main features of human chronic phase CML.

This allows us to considerably improve on the phenotypic and functional characterization of CML-LSCs, and to segregate them from two newly identified nonself-renewing leukemic multipotent progenitor populations that are present in the LSK fraction of the BM. These results unambiguously prove the long-standing concept that CML arise from transformed HSCs, and demonstrate that the clinically relevant CML-LSCs are solely contained in the rare LT-HSC compartment. This finding is essential to identify therapeutic targets that are specific to CML-LSCs and not to the most abundant leukemic multipotent progenitors, as currently done with the loose LSK definition of CML-LSCs. Moreover, we describe how leukemic multipotent progenitors contribute to CML development, and the essential function played by the protumorigenic inflammatory environment in controlling disease pathogenesis.

CML-LSCs

Here, we demonstrate that CML-LSCs are exclusively contained in the rare LT-HSC compartment, which represent <10% of the LSK BM fraction (Warr et al., 2011). This level of resolution allows us to investigate the aberrant features that are specific to CML-LSCs, and to identify key deregulated mechanisms that could be amenable to targeted therapy. Based on phenotypic analysis and serial transplantation of *BCR/ABL*-expressing LSK cells, it

IL-6 protein secreted in the culture supernatant (Figure 8B). We then investigated TKI-treated K562 cells for expression of a panel of effectors genes known to regulate *IL-6* expression (Figure 8C). We found a significant downregulation of both *LIN28* and *LIN28b* expression and a considerable increase in *BCL6* expression. *BCL6* is a direct transcriptional repressor of the *IL-6* gene (Yu et al., 2005), and recent work has shown that BCR/ABL-driven STAT5 activation inhibits *BCL6* expression (Duy et al., 2011). Although the regulation of *LIN28/28b* by BCR/ABL is still largely unknown, they have been shown to inhibit the maturation of the *Let-7* microRNA, which is itself a negative regulator of *IL-6* expression (Iliopoulos et al., 2009). Therefore, we propose that pharmacological inhibition of BCR/ABL activity increased *BCL6* levels and, as shown here, decreased *LIN28/28b* levels (Figure 8C), which could both contribute to the downregulation of *IL-6* expression observed in TKI-treated K562 cells (Figure 8D). *BCR/ABL* levels have also been shown to increase with disease progression (Savona and Talpaz, 2008) and elevated levels of IL-6 protein have been observed in the serum of accelerated and myeloid blasts crisis patients (Anand et al., 1998). Consistently, we observed a striking upregulation of *IL-6* expression during CML development in a large cohort of chronic, accelerated and blast crisis phase CML samples analyzed by microarray (Figure 8E). Furthermore, we noticed an accompanying decrease

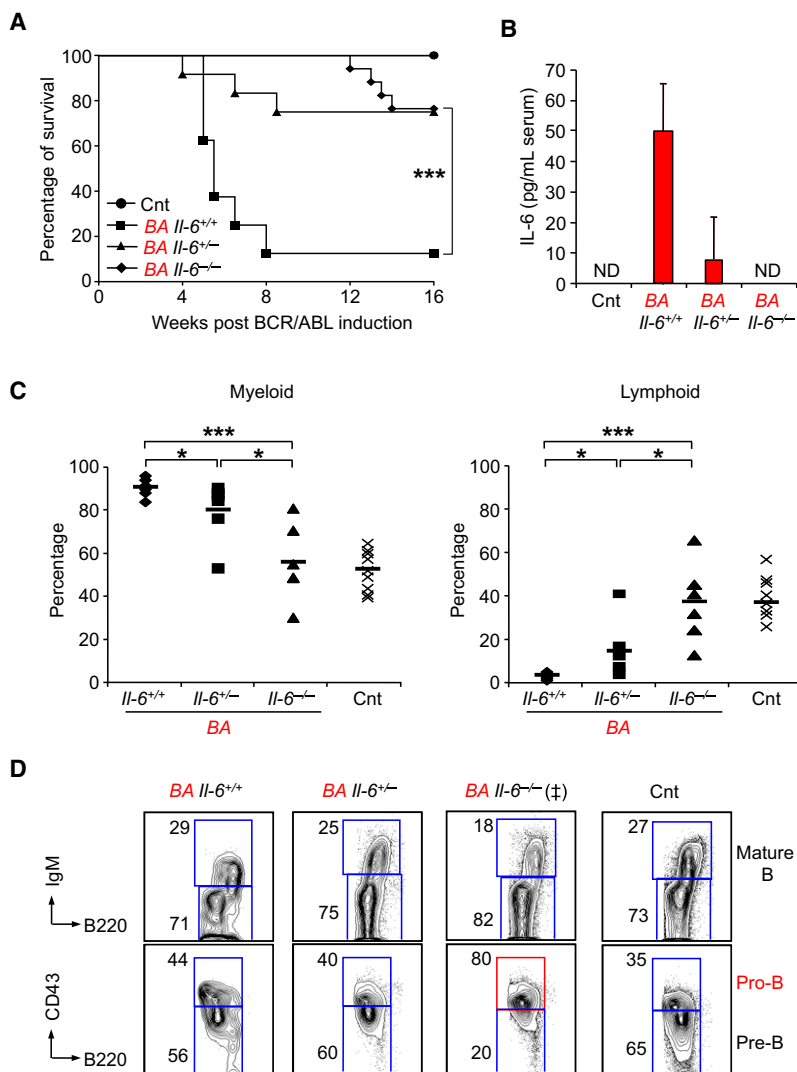


Figure 7. Role of IL-6 in CML Development

(A) Survival curve of Cnt (n = 11) and *Il-6*^{+/+} (n = 11), *Il-6*^{+/-} (n = 12), and *Il-6*^{-/-} (n = 17) BA mice after doxycycline withdrawal (*p ≤ 5 × 10⁻²).

(B) ELISA measurement of serum IL-6 levels in Cnt and *Il-6*^{+/+}, *Il-6*^{+/-}, and *Il-6*^{-/-} BA mice. Results are expressed as mean ± SEM (n = 7). ND, not detectable.

(C) Percentage of Mac1⁺ myeloid (left) and B220⁺ B-lymphoid (right) cells in BM of individual control and *Il-6*^{+/+}, *Il-6*^{+/-}, and *Il-6*^{-/-} BA mice (n = 5–10; *p ≤ 5 × 10⁻², ***p ≤ 5 × 10⁻⁴).

(D) Representative FACS plots showing the phenotype of B cell progenitors generated in Cnt and *Il-6*^{+/+}, *Il-6*^{+/-}, and *Il-6*^{-/-} BA mice. ‡Indicates that FACS plots is representative of three out of five analyzed mice with this genotype.

recent findings in the *junB*-deficient CML-like model, where increase proliferation in transformed LT-HSCs is also not associated with a loss of self-renewal capacity (Santaguida et al., 2009). Consistent with this idea, BCR/ABL activity does not dramatically disrupt the transcriptional networks regulating LT-HSC self-renewal. More strikingly, we observe significant changes in cell cycle machinery and decrease expression of Notch signaling components in BCR/ABL-expressing LT-HSCs that are similar to the deregulations we previously described in *junB*-deficient LT-HSCs (Santaguida et al., 2009). These findings reinforce the idea that deregulation of the Notch pathway is a key contributor to aberrant myelopoiesis (Klinakis et al., 2011), and that loss of quiescence and resulting hyperproliferation in transformed LT-HSCs may occur through a dampening of the cyclin D1/Cdkn1c (p57) regulatory axis (Pietras et al., 2011). They also suggest that LT-HSC transformation may, in fact, result from the perturbation of a few common regulatory pathways regard-

less of the initiating oncogenic event and that strategy aimed at restoring Notch activity in transformed LT-HSCs may represent a valid therapeutic approach to targeted LSC aberrant activity in CML and other type of MPNs.

has been recently suggested that BCR/ABL activity induces loss of HSC self-renewal capacity and promotes differentiation (Schemionek et al., 2010). Indeed, we observe a profound reorganization of the LSK BM compartment following CML development, with a severe reduction in the numbers LT-HSCs, ST-HSCs, and expansion of nonself-renewing LSK/Fik2⁻/CD48⁺ cells and Fik2⁺ MPPs. However, we find that such changes in the BM are associated with the development of a massive myelofibrosis, and are fully compensated for by the emergence of extramedullary hematopoiesis with increased numbers of LT-HSCs in the spleen. Most importantly, we observe that BCR/ABL-expressing LT-HSCs are able to self-renew extensively and to out-compete normal LT-HSCs, both in stress conditions upon transplantation in sublethally irradiated recipients, and in steady-state conditions when BCR/ABL expression is induced in transplanted mice harboring chimeric hematopoiesis. This property is consistent with the clonal dominance observed in human CML patients, where the majority of CD34⁺ stem and progenitor cells carry the BCR/ABL translocation (Holyoake et al., 1999). These findings are also in line with our

less of the initiating oncogenic event and that strategy aimed at restoring Notch activity in transformed LT-HSCs may represent a valid therapeutic approach to targeted LSC aberrant activity in CML and other type of MPNs.

CML Multipotent Progenitors

Here, we also demonstrate that BCR/ABL expression affects the activity of ST-HSCs and MPPs, but not of any other tested lineage-committed progenitors. BCR/ABL activity increases cell cycling and considerably expands the output of both ST-HSCs and MPPs, thereby providing these leukemic progenitors with extensive, although transient, in vivo reconstitution ability upon transplantation. Strikingly, opposite lineage outputs were generated from these transplanted cells, with leukemic ST-HSCs, like CML-LSCs, giving rise to a generalized myeloid hyperplasia, and leukemic MPPs producing a massive accumulation of pro-B cells in the BM. These results indicate that BCR/ABL exerts cell-type specific effects and biases the lineage potential of specific multipotent progenitor cells based on their stage of maturation and, likely, the permissiveness of their

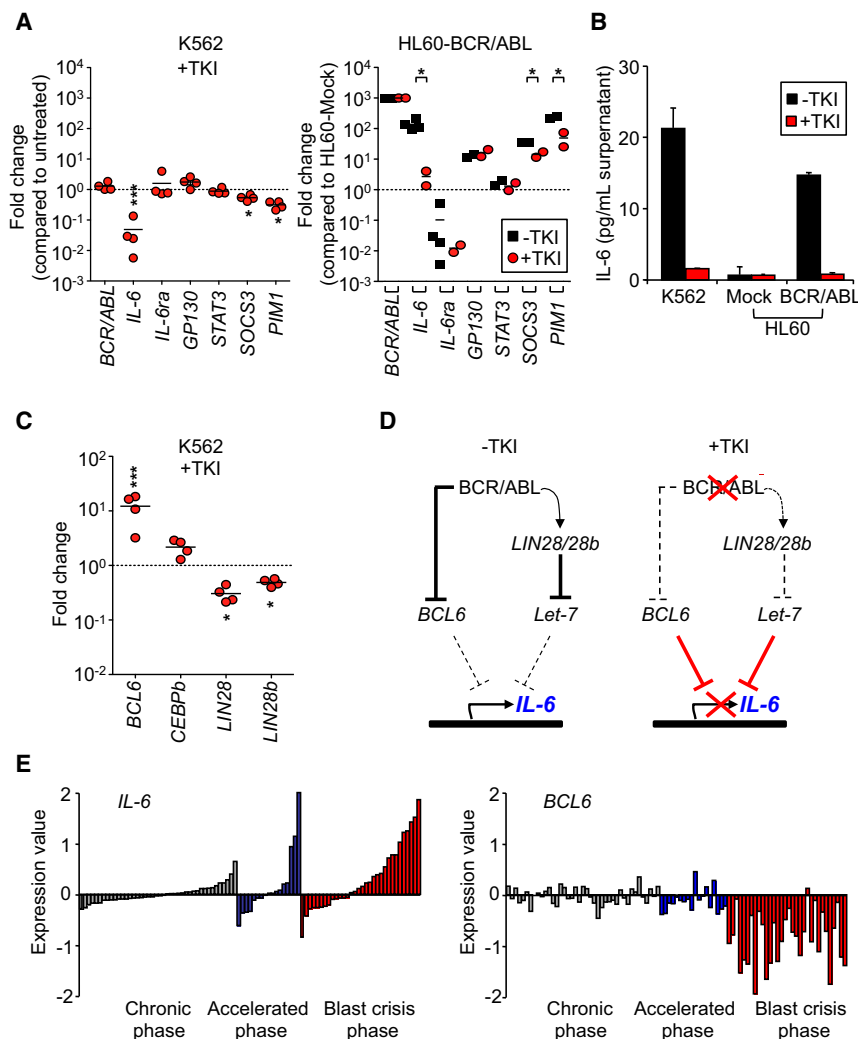


Figure 8. BCR/ABL Controls IL-6 Expression

(A) BCR/ABL-dependent IL-6 expression in human cell lines. qRT-PCR analysis of IL-6 pathway components in K562 (left) and BCR/ABL-expressing HL60 (right) cells with or without TKI treatment. Results (mean; $n = 2-4$) are expressed as fold change relative to untreated K562 (left) or Mock-transfected HL60 (right) cells (mean; $n = 2-4$; * $p < 0.05$).

(B) ELISA measurement of IL-6 concentration in the supernatant of the cell lines used in (A). Results are expressed as mean \pm SEM ($n = 2$).

(C) qRT-PCR analysis of BCR/ABL signaling pathway components in K562 cells with or without TKI treatment. Results (mean; $n = 4$) are expressed as fold change relative to untreated K562 cells.

(D) Proposed model for BCR/ABL regulation of IL-6 expression. In CML cells, BCR/ABL stimulates LIN28 production, which in turn blocks Let-7 microRNA maturation (Iliopoulos et al., 2009) and/or blocks BCL6 expression (Duy et al., 2011) hence allowing transcription of the IL-6 gene. Inhibition of BCR/ABL activity by TKI treatment reduces LIN28 expression and/or releases BCL6 expression hence allowing them to block IL-6 expression (Yu et al., 2005).

(E) Expression of IL-6 ($p < 0.05$) and BCL6 ($p < 0.0001$) in BM or PB from chronic (gray), accelerated (blue), and blast crisis (red) phase CML patients relative to the expression in a pool of 200 chronic phase patients. Expression is in logarithmic scale. Data was analyzed using Qlucore Omics Explorer (Qlucore, AB, Lund, Sweden). The software performs a multigroup comparison using the ANOVA F-test.

molecular programming. These results highlight the fact that CML develops from transformed LT-HSCs through a continuum of leukemic progenitor cells that are devoid of self-renewal activity but have defined aberrant properties. As we observe here, such nonself-renewing leukemic progenitors can easily kill a mouse when transplanted at high doses and generate a disease, which despite being not transplantable, closely mimics CML both in kinetic and phenotype. This can have a confusing effect especially when transplanting high numbers of transduce mix populations such as 5-FU treated BM or LSK cells. Caution should therefore be taken in interpreting the results of retroviral transduction/transplantation experiments, particularly when assessing the effect on CML-LSC numbers through serial transplantations, and on the myeloid/lymphoid nature of the emerging disease.

Protumorigenic Inflammatory Environment in CML Pathogenesis

Our results unveil an essential paracrine mechanism involving the proinflammatory cytokine IL-6, which serves as a positive feedback loop to sustain CML development and acts at the level

of leukemic MPPs by reprogramming them toward myeloid development at the expense of their intrinsic BCR/ABL-driven lymphoid-bias potential. CML development is accompanied by considerable changes in the proinflammatory tumor environment. Autocrine or paracrine mechanisms involving IL-3, G-CSF or GM-CSF have been reported to enhance the proliferation and viability of primitive CML cells both in mouse models and human samples (Jiang et al., 1999; Zhang and Ren, 1998). However, the real contribution of these pathways to CML development remains unclear as their inactivation in the mouse does not significantly affect disease outcome (Li et al., 2001). Here, we identify IL-6 as a key cytokine whose expression and secretion by myeloid cells is most affected by CML development, which confirms earlier findings in serum of CML patients (Anand et al., 1998) and very recent observations using the retroviral transduction/transplantation model of CML (Schmidt et al., 2011). IL-6 exerts multiple, and some time divergent, functions on hematopoietic cells, including the provision of instructive cues for myeloid differentiation in normal contexts and in mouse models of inflammation or autoimmune diseases (Maeda et al., 2005, 2009). Here, we show that the IL-6 receptor expression starts at the MPP stage of hematopoietic differentiation and is not affected by BCR/ABL activity. We demonstrate that IL-6 acts on both normal and

leukemic MPPs to redirect their differentiation potential toward the myeloid lineage at the expense of lymphoid differentiation. Furthermore, we show unambiguously by a genetic approach in the mouse that impairment of IL-6 signaling delays CML development, hence confirming the essential contribution of this pathway as a feedback loop supporting chronic phase CML. This paracrine mechanism appears exacerbated in CML myeloid blast crisis, most likely due to increased IL-6 production by blast cells as shown here by genome-wide genes expression analyses of CML patient samples. Disruption of the IL-6 paracrine loop, either through mutations in the IL-6 signaling pathway or loss of IL-6 production, and subsequent release of CML-MPP intrinsic B-lymphoid potential may also constitute the first step in the otherwise apparently random myeloid/lymphoid conversion observed during CML progression to lymphoid blast crisis. Instructive signals controlling the myeloid/lymphoid balance in CML is reminiscent to what has been described in MLL-rearranged AML, where growth factors and cytokines can instruct the lineage fate of multipotent LSCs (Barabé et al., 2007). Taken together, these findings demonstrate that blood cancers, like solid cancers, are profoundly affected by the protumorigenic inflammatory environment in which leukemic stem and progenitor cells reside and function.

IL-6 Signaling As a Target for CML Therapy

IL-6 has been previously implicated in the pathogenesis of hematological malignancies (i.e., multiple myeloma, Hodgkin's lymphoma) and solid cancers (i.e., breast, prostate, and recently, pancreatic cancers) (Hong et al., 2007). Here, we identify IL-6 as a major player in CML pathogenesis. We demonstrate that BCR/ABL activity dictates the level of IL-6 produced by both mouse and human myeloid CML cells. We show that BCR/ABL regulates *IL-6* mRNA levels through a complex and indirect mechanism involving, at least, BCL6 and the LIN28/28b-Let-7 pathway, which are two known transcriptional regulators of the *IL-6* gene (Iliopoulos et al., 2009; Yu et al., 2005). We find that pharmacological inhibition of BCR/ABL activity with TKIs restore *IL-6* expression and production to its normally low levels. We also show that disruption of the IL-6 paracrine loop through genetic ablation of the *IL-6* gene in mice significantly delays CML onset despite persistent BCR/ABL activity. These results suggest that therapies aimed at blocking IL-6 or targeting the IL-6 signal transduction pathway, although noncurative, could provide clinical benefits for CML patients that develop resistance to TKI treatment or undergo myeloid blast crisis progression. One important concern is that the aberrant B cell expansion driven by CML-MPPs and observed upon IL-6 inactivation may represent a preleukemic stage, which could evolve into an aggressive B-ALL upon acquisition of additional mutations (Mullighan et al., 2008). However, no lymphoid malignancies have spontaneously developed over time in aged *BA IL-6^{-/-}* mice ($n = 17$; data not shown), and we are currently performing additional genetic experiments in *BA IL-6^{-/-}* mice to directly test this hypothesis and address the safety of IL-6 blocking therapies. Finally, it is tempting to speculate that such self-reinforcing paracrine loop involving IL-6, or other secreted proinflammatory factors, might be relevant in a broad spectrum of myeloid disorders. It opens the possibility of combinatorial strategies targeting not only the bulk tumor cells and the LSC compartment but also the pro-

morigenic inflammatory environment, which controls the function of the leukemic hierarchy. Such a three-pronged approach might, in fact, be needed to develop curative treatment for CML and other types of blood malignancies.

EXPERIMENTAL PROCEDURES

Mice

Scf/Tal-1-tTA and *TRE-BCR/ABL* mice were backcrossed for at least nine generations in the C57Bl/6 background and were interbred in presence of 20 mg/l doxycycline (Sigma-Aldrich) in their drinking water. *IL-6^{-/-}* mice were purchased from the Jackson laboratory. Transplantations were performed as previously described (Santaguida et al., 2009). All animal experiments were performed in accordance with UCSF IACUC approved protocols.

Flow Cytometry

Staining and enrichment procedures for stem and progenitor population sorting and analysis were performed as previously described (Santaguida et al., 2009). Cells were sorted or analyzed on a FACS ARIAll or LSRII (Becton Dickinson), respectively.

Cell Culture

For myeloid differentiation assays, 500 MPPs or GMPs were plated in 10 mm dishes in methylcellulose (StemCell Technology, M3231) supplemented with SCF (25 ng/ml) and Flt3L (25 ng/ml) in the presence or absence of IL-6 (20 ng/ml) (Peprotech) and grown for 2 weeks. For B cell differentiation assays, cells were plated on OP9 stromal cells in OptiMEM medium (Invitrogen) supplemented with 5% FBS (StemCell Technology), SCF (10 ng/ml), Flt3L (10 ng/ml), and IL-7 (5 ng/ml). Following sequential withdrawal of Flt3L and SCF upon 2-day intervals, cultures were maintained in IL-7 and analyzed at day 8 by flow cytometry. K562 and HL60 human cell lines were cultured for 15–20 hr in RPMI medium supplemented with 10% FBS in presence or absence of TKI (5 μ M Imatinib or 100 nM Dasatinib).

Protein Array and ELISA

Antibody-based protein array (Proteome Profiler, R&D Systems) and IL-6 ELISA assays (eBioscience) were performed on sera according to the manufacturer's instructions. The assay detection range was 5–1000 pg/ml.

Proliferation Assays

Intracellular BrdU staining and 7AAD/Pyronin Y staining were performed as previously described (Santaguida et al., 2009).

Quantitative RT-PCR Array

Quantitative RT-PCR arrays were performed on the Fluidigm 96.96 Dynamic Array IFC platform. Intron-spanning sets of primers for preamplification and quantitative PCR were validated on serial dilution of total mouse cDNA to ensure linear amplification, PCR specificity, and performance. One hundred cells were directly sorted in 5 μ l of resuspension buffer from CellDirect One-Step qRT-PCR kits (Invitrogen). Samples were used for random hexamer-based reverse-transcription (SuperScript III kit, Invitrogen) and preamplified for 18 cycles with Platinum Taq DNA polymerase (Invitrogen) and primer mix (50 nM). Resulting cDNA products were analyzed on Fluidigm BioMark System using EvaGreen dye (Biotium). Each measurement was performed in triplicate and expression levels of *Gusb*, *Gapdh*, *Pgk1*, and *Ctfc* housekeeping genes were used for normalization.

Microarray Gene Expression Studies

Gene expression profiles of CML patient samples have been described previously (Radich et al., 2006; GEO accession number 4170). This published data set was analyzed for the expression of IL-6 and BCL6 in BM and PB samples from 42 chronic, 17 accelerated, and 32 blast crisis phase CML patients.

Statistics

All the data are expressed as mean \pm standard error of the mean (error bar) except when indicated. The p values were generated using unpaired Student's t test and considered significant when ≤ 0.05 . For survival curve, p values were

generated using Mantel-Cox test. N indicates the numbers of independent experiments performed.

SUPPLEMENTAL INFORMATION

Supplemental Information includes three figures and can be found with this article online at doi:10.1016/j.ccr.2011.10.012.

ACKNOWLEDGMENTS

We thank the members of the Passequé laboratory for critical reading of this manuscript; Dr. S. Kogan (UCSF) for help with histological analyses; Dr. N.P. Shah (UCSF) for providing the human cell lines; Dr. D. Tenen (Harvard University) for the generous gift of the *Scl/Tal-1-tTA* and *TRE-BCR/ABL* mice; K. Livak and A. Hamilton (Fluidigm) for expert assistance with QPCR analyses; T. Rambaldo and B. Hyun for management of our Flow Cytometry core facility; and the members of the UCSF Hematological Malignancy group for discussion and support. This work was supported by a Rita Allen Scholar award and NIH grant HL092471 to E.P.

Received: March 2, 2011

Revised: August 9, 2011

Accepted: October 13, 2011

Published: November 14, 2011

REFERENCES

- Anand, M., Chodda, S.K., Parikh, P.M., and Nadkarni, J.S. (1998). Abnormal levels of proinflammatory cytokines in serum and monocyte cultures from patients with chronic myeloid leukemia in different stages, and their role in prognosis. *Hematol. Oncol.* 16, 143–154.
- Barabé, F., Kennedy, J.A., Hope, K.J., and Dick, J.E. (2007). Modeling the initiation and progression of human acute leukemia in mice. *Science* 316, 600–604.
- Barnes, D.J., and Melo, J.V. (2006). Primitive, quiescent and difficult to kill: the role of non-proliferating stem cells in chronic myeloid leukemia. *Cell Cycle* 5, 2862–2866.
- Benveniste, P., Frelin, C., Janmohamed, S., Barbara, M., Herrington, R., Hyam, D., and Iscove, N.N. (2010). Intermediate-term hematopoietic stem cells with extended but time-limited reconstitution potential. *Cell Stem Cell* 6, 48–58.
- Buesche, G., Ganser, A., Schlegelberger, B., von Neuhoff, N., Gadzicki, D., Hecker, H., Bock, O., Frye, B., and Kreipe, H. (2007). Marrow fibrosis and its relevance during imatinib treatment of chronic myeloid leukemia. *Leukemia* 21, 2420–2427.
- Corbin, A.S., Agarwal, A., Loriaux, M., Cortes, J., Deininger, M.W., and Druker, B.J. (2011). Human chronic myeloid leukemia stem cells are insensitive to imatinib despite inhibition of BCR-ABL activity. *J. Clin. Invest.* 121, 396–409.
- Duy, C., Hurtz, C., Shojaaee, S., Cerchietti, L., Geng, H., Swaminathan, S., Klemm, L., Kweon, S.M., Nahar, R., Braig, M., et al. (2011). BCL6 enables Ph+ acute lymphoblastic leukaemia cells to survive BCR-ABL1 kinase inhibition. *Nature* 473, 384–388.
- Holyoake, T., Jiang, X., Eaves, C., and Eaves, A. (1999). Isolation of a highly quiescent subpopulation of primitive leukemic cells in chronic myeloid leukemia. *Blood* 94, 2056–2064.
- Hong, D.S., Angelo, L.S., and Kurzrock, R. (2007). Interleukin-6 and its receptor in cancer: implications for translational therapeutics. *Cancer* 110, 1911–1928.
- Hu, Y., Swerdlow, S., Duffy, T.M., Weinmann, R., Lee, F.Y., and Li, S. (2006). Targeting multiple kinase pathways in leukemic progenitors and stem cells is essential for improved treatment of Ph+ leukemia in mice. *Proc. Natl. Acad. Sci. USA* 103, 16870–16875.
- Huntly, B.J., Shigematsu, H., Deguchi, K., Lee, B.H., Mizuno, S., Duclos, N., Rowan, R., Amaral, S., Curley, D., Williams, I.R., et al. (2004). MOZ-TIF2, but not BCR-ABL, confers properties of leukemic stem cells to committed murine hematopoietic progenitors. *Cancer Cell* 6, 587–596.
- Iliopoulos, D., Hirsch, H.A., and Struhl, K. (2009). An epigenetic switch involving NF-kappaB, Lin28, Let-7 MicroRNA, and IL6 links inflammation to cell transformation. *Cell* 139, 693–706.
- Jiang, X., Lopez, A., Holyoake, T., Eaves, A., and Eaves, C. (1999). Autocrine production and action of IL-3 and granulocyte colony-stimulating factor in chronic myeloid leukemia. *Proc. Natl. Acad. Sci. USA* 96, 12804–12809.
- Klinakis, A., Lobry, C., Abdel-Wahab, O., Oh, P., Haeno, H., Buonamici, S., van De Walle, I., Cathelin, S., Trimarchi, T., Araldi, E., et al. (2011). A novel tumour-suppressor function for the Notch pathway in myeloid leukaemia. *Nature* 473, 230–233.
- Kopf, M., Baumann, H., Freer, G., Freudenberg, M., Lamers, M., Kishimoto, T., Zinkernagel, R., Bluethmann, H., and Köhler, G. (1994). Impaired immune and acute-phase responses in interleukin-6-deficient mice. *Nature* 368, 339–342.
- Koschmieder, S., Göttgens, B., Zhang, P., Iwasaki-Arai, J., Akashi, K., Kutok, J.L., Dayaram, T., Geary, K., Green, A.R., Tenen, D.G., and Huettner, C.S. (2005). Inducible chronic phase of myeloid leukemia with expansion of hematopoietic stem cells in a transgenic model of BCR-ABL leukemogenesis. *Blood* 105, 324–334.
- Li, S., Gillissen, S., Tomasson, M.H., Dranoff, G., Gilliland, D.G., and Van Etten, R.A. (2001). Interleukin 3 and granulocyte-macrophage colony-stimulating factor are not required for induction of chronic myeloid leukemia-like myeloproliferative disease in mice by BCR/ABL. *Blood* 97, 1442–1450.
- Maeda, K., Malykhin, A., Teague-Weber, B.N., Sun, X.H., Farris, A.D., and Coggeshall, K.M. (2009). Interleukin-6 aborts lymphopoiesis and elevates production of myeloid cells in systemic lupus erythematosus-prone B6.Sle1.Yaa animals. *Blood* 113, 4534–4540.
- Maeda, K., Baba, Y., Nagai, Y., Miyazaki, K., Malykhin, A., Nakamura, K., Kincade, P.W., Sakaguchi, N., and Coggeshall, K.M. (2005). IL-6 blocks a discrete early step in lymphopoiesis. *Blood* 106, 879–885.
- Mullighan, C.G., Miller, C.B., Radtke, I., Phillips, L.A., Dalton, J., Ma, J., White, D., Hughes, T.P., Le Beau, M.M., Pui, C.H., et al. (2008). BCR-ABL1 lymphoblastic leukaemia is characterized by the deletion of Ikaros. *Nature* 453, 110–114.
- Passequé, E., and Weisman, I.L. (2005). Leukemic stem cells: where do they come from? *Stem Cell Rev.* 1, 181–188.
- Perrotti, D., Jamieson, C., Goldman, J., and Skorski, T. (2010). Chronic myeloid leukemia: mechanisms of blastic transformation. *J. Clin. Invest.* 120, 2254–2264.
- Pietras, E.M., Warr, M., and Passequé, E. (2011). Cell cycle regulation in hematopoietic stem cells. *J. Cell Biol.*, in press.
- Porosnicu, M., Nimmanapalli, R., Nguyen, D., Worthington, E., Perkins, C., and Bhalla, K.N. (2001). Co-treatment with As2O3 enhances selective cytotoxic effects of STI-571 against Bcr-Abl-positive acute leukemia cells. *Leukemia* 15, 772–778.
- Radich, J.P., Dai, H., Mao, M., Oehler, V., Schelter, J., Druker, B., Sawyers, C., Shah, N., Stock, W., Willman, C.L., et al. (2006). Gene expression changes associated with progression and response in chronic myeloid leukemia. *Proc. Natl. Acad. Sci. USA* 103, 2794–2799.
- Santaguida, M., Schepers, K., King, B., Sabnis, A.J., Forsberg, E.C., Attema, J.L., Braun, B.S., and Passequé, E. (2009). JunB protects against myeloid malignancies by limiting hematopoietic stem cell proliferation and differentiation without affecting self-renewal. *Cancer Cell* 15, 341–352.
- Savona, M., and Talpaz, M. (2008). Getting to the stem of chronic myeloid leukaemia. *Nat. Rev. Cancer* 8, 341–350.
- Schemionek, M., Elling, C., Steidl, U., Bäumer, N., Hamilton, A., Spieker, T., Göthert, J.R., Stehling, M., Wagers, A., Huettner, C.S., et al. (2010). BCR-ABL enhances differentiation of long-term repopulating hematopoietic stem cells. *Blood* 115, 3185–3195.
- Schmidt, T., Kharabi Masouleh, B., Loges, S., Cauwenberghs, S., Fraisl, P., Maes, C., Jonckx, B., De Keersmaecker, K., Kleppe, M., Tjwa, M., et al. (2011). Loss or inhibition of stromal-derived PIGF prolongs survival of mice with imatinib-resistant Bcr-Abl1(+) leukemia. *Cancer Cell* 19, 740–753.
- Viswanathan, S.R., Powers, J.T., Einhorn, W., Hoshida, Y., Ng, T.L., Toffanin, S., O'Sullivan, M., Lu, J., Phillips, L.A., Lockhart, V.L., et al. (2009). Lin28

promotes transformation and is associated with advanced human malignancies. *Nat. Genet.* **41**, 843–848.

Warr, M.R., Pietras, E.M., and Passegue, E. (2011). Mechanisms controlling hematopoietic stem cell functions during normal hematopoiesis and hematological malignancies. *Wiley Interdiscip. Rev. Syst. Biol. Med.* **6**, 681–701.

Yu, R.Y., Wang, X., Pixley, F.J., Yu, J.J., Dent, A.L., Broxmeyer, H.E., Stanley, E.R., and Ye, B.H. (2005). BCL-6 negatively regulates macrophage proliferation by suppressing autocrine IL-6 production. *Blood* **105**, 1777–1784.

Zhang, B., Strauss, A.C., Chu, S., Li, M., Ho, Y., Shiang, K.D., Snyder, D.S., Huettner, C.S., Shultz, L., Holyoake, T., and Bhatia, R. (2010). Effective targeting of quiescent chronic myelogenous leukemia stem cells by histone deacetylase inhibitors in combination with imatinib mesylate. *Cancer Cell* **17**, 427–442.

Zhang, X., and Ren, R. (1998). Bcr-Abl efficiently induces a myeloproliferative disease and production of excess interleukin-3 and granulocyte-macrophage colony-stimulating factor in mice: a novel model for chronic myelogenous leukemia. *Blood* **92**, 3829–3840.